Controlling Polymer Architecture to Design Dynamic Network Materials with Multiple Dynamic Linkers

Jafer R. Vakil,[a] Nethmi De Alwis Watuthanthrige,[a] Zachary A. Digby,[a] Borui Zhang,[a] Hannah A. Lacy,[a] Jessica L. Sparks,[b] Dominik Konkolewicz[a,*]

a Department of Chemistry and Biochemistry, Miami University, 651 E High St. Oxford, OH, 45056, USA

b Department of Chemical Paper and Biomedical Engineering, Miami University, 650 E High St. Oxford, OH, 45056, USA

* corresponding author: d.konkolewicz@miamiOH.edu

Abstract. A one pot synthesis is applied to control the chain structure and architecture of multiply dynamic polymers, with this allowing fine tuning of materials properties by choice of polymer chain length or crosslink density. Macromolecules containing both non-covalent linkers based on quadruple hydrogen-bonded 2-(((6-(3-(6-methyl-4-oxo-1,4-dihydropyrimidin-2-yl)ureido)hexyl)carbamoyl)oxy)ethyl methacrylate (UPyMA), and thermoresponsive dynamic covalent furan-maleimide based Diels-Alder linkers are explored. The primary polymer's architecture was controlled by reversible addition-fragmentation chain transfer (RAFT) polymerization, with the dynamic non-covalent (UPyMA) and dynamic covalent furfuryl methacrylate (FMA) units incorporated into the same backbone. The materials are crosslinked, taking advantage of the "click" chemistry properties of the furan-maleimide reaction. The polymer materials showed stimulus-responsive thermomechanical properties with a decrosslinking temperature increasing with the polymer's primary chain length and crosslink density. The polymers had good thermally promoted self-healing properties due to the dynamic

covalent Diels-Alder bonds. Besides, the materials had excellent stress relaxation characteristics induced by the exchange of the hydrogen bonds in UPyMA units.

Introduction.

Dynamic chemistry is characterized by the ability of a bond or adduct to break or reform either autonomously or in response to stimuli.[1] Recently, polymer systems employing dynamic linkers have gained attention due to the functionalities afforded by their dynamic bonds, including self-healing, shape-memory, degradability, adaptability, and malleability.[1–11] Most dynamic crosslinkers can be classified as either non-covalent or covalent linkers. While non-covalent linkers typically offer autonomous exchange under ambient conditions, the strength of the non-covalent interactions and relatively rapid exchange rates often render the materials containing dynamic non-covalent bonds susceptible to creep.[12–19] Dynamic covalent linkers typically exchange slowly enough to allow for creep resistant materials. However, they are often incapable of exhibiting self-healing, or stress relaxation without the application of external stimuli such as heat, light, or pH.[12,20,21] Hence, the benefits and drawbacks of covalent and non-covalent crosslinkers are almost complementary. A solution is to employ both covalent and non-covalent crosslinkers in a polymer system for superior mechanical performance.

Dynamic non-covalent adducts and bonds include linkages based on hydrogen bonds, metal coordination, hydrophobic interactions, guest-host interactions, ionic interactions, and materials utilizing such interactions have been successfully implemented within polymeric systems to enhance mechanical strength and performance.[22–24] Noncovalent interactions based on hydrogen bonds have received particular attention. For example, the 2-ureido-4-pyrimidone (UPy) group has strong dimerization through a quadruple hydrogen bond structure, and has seen use in biopolymers and supramolecular polymers.[25–28] Polymerizable derivatives of the UPy moiety

such as 2-(((6-(3-(6-methyl-4-oxo-1,4-dihydropyrimidin-2-yl)ureido)hexyl)carbamoyl)oxy)ethyl acrylate (UPyA) and 2-(((6-(3-(6-methyl-4-oxo-1,4-dihydropyrimidin-2-yl)ureido)hexyl)carbamoyl)oxy)ethyl methacrylate (UPyMA) can also exhibit high dimerization and have been used to make complex materials including interpenetrating networks where one network is linked through UPy hydrogen bonds.[29–31] Likewise, a covalent dynamic linker which has seen much success in polymer networks is that of the Diels-Alder reaction. Typically, the Diels-Alder process reversibly forms a six-membered ring from a diene and a dienophile via [4 + 2] cycloaddition, and has been implemented in many self-healing materials.[32–41] The Diels-Alder reaction satisfies the "click" criteria, hence the reaction's ease of use and tolerance to functionality makes it an excellent candidate for use as a covalent dynamic linker.[42–44] Free radical polymerization in tandem with the Diels-Alder reaction has, in the past, resulted in industrial-scale synthesis of polymers. However, conventional free radical polymerization occurs at the expense of controlled polymer structure, leading to poorly defined primary polymers and limited control over material properties.

Traditional approaches towards polymer synthesis include step-growth polymerization, where monomers react in succession to form oligomers which grow to polymers, or chain-growth polymerization, where monomers react with an active site on a chain. However, traditional step-growth and radical chain growth reactions give polymers of high molar mass dispersity ($M_w/M_n \gtrsim 2$). In an effort to construct and tune molecular parameters, several reversible deactivation radical polymerization methods have been developed, such as reversible-addition fragmentation chain-transfer polymerization (RAFT). Mechanistically, RAFT occurs via the degenerative exchange of a radical and a thiocarbonylthio chain transfer agent.[45,46] RAFT has tolerance to a diverse range of functional monomers, giving a polymer with narrow dispersity

($M_w/M_n < 1.5$, and often $M_w/M_n < 1.2$) and good control over polymer chain length and microstructure.[47–50]

Although dynamic and multiply dynamic materials have been developed in the past,[51] the expansion of dynamic controlled architecture will allow for the development of precision materials with powerful properties for applications such as sealants, coatings, elastomers, and shape-memory materials.[29,31,52,53] Zhang *et al.* utilized RAFT polymerization to synthesize and tune interpenetrating networks (IPN) with success.[29,52]This approach was then adapted to IPN materials of different polarity, finding that non-polar poly(ethyl acrylate)-based matrices promote strong UPy association constants and enhance toughness, compared to polar poly(2-hydroxyethyl acrylate)-based matrices.[52] A drawback of IPNs is that they require a two-pot or two-step synthesis, when the same backbone is used for both networks.[29,31] Alternatively, when different backbones are used in a dynamic network, there is the risk of phase separation if the two networks are immiscible.

In this paper, a simple one-pot polymer synthesis approach was applied to make networks where all linkers are on the same backbone. This type of network architecture is referred to as a single network (SN). In a SN all crosslinkers are in the same network, although there may be more than one type of linker in the material. RAFT polymerization was used to control the parameters of molecular systems, utilizing poly(ethyl acrylate) (PEA) as the polymer backbone with UPyMA hydrogen-bonded linkers and covalent furfuryl methacrylate (FMA) crosslinkers. This work expands on preliminary SN polymer synthesis via a one-pot reaction and then crosslinks the polymers with a bismaleimide compound to make SN materials with two dynamic linkers.[29] RAFT allows the polymer microstructure, the crosslinker content or placement, and the polymer chain length to be tailored to a given application. This paper expands upon the earlier

synthesis and explores the impact of macromolecular architecture on the mechanical, self-healing, and stress-relaxation properties of polymer materials containing both hydrogen-bonded and dynamic covalent linkers in these SN type materials. The synthesized materials can achieve over 95% recovery of mechanical properties after self-healing at elevated temperatures, and by carefully choosing the polymer structure, strong materials with tensile peak stress of up to 2 MPa were obtained.

Experimental.

Materials

All materials were obtained from commercial suppliers unless otherwise stated. All materials were used as received unless noted otherwise. Ethyl acrylate (EA, 99%), dibutyl tin(II) dilaurate (99%), 2-amino-4-hydroxy-6-methylpyrimidine (98%), 1,1′-(methylenedi-4,1-phenylene) bismaleimide (BMI, 95%), 2,2′-Azobis(2-methylpropionitrile) (AIBN, 98%) were obtained from Sigma Aldrich. Furfuryl alcohol (98%) was obtained from Alfa Aesar. N,N-dimethylformamide (DMF, 99.5%), methacrylic acid (99%), 2-hydroxyethyl methacrylate (>95%) and 1-dodecantthiol(DDT, 95%) were obtained from TCI America. 1,6-diisocyanteohexane (99+%) and 2- bromopropionic acid (99+%) were obtained from Acros Organics. Carbon disulfide (99%) and sodium hydroxide (>95%) were obtained from Fisher Scientific. 1-Ethyl-3-(3-dimethylaminopropyl)carbodiimide hydrochloride (EDC, 98%) was obtained from BioSynth-CarboSynth.

Synthesis of (2-propionic acid)yldodecyl trithiocarbonate (PADTC)

(2-Propionic acid)yldodecyl trithiocarbonate (PADTC) was synthesized following the literature, and the product was confirmed by the ^{1}H-NMR in agreement with the literature (Figure S1).[54] ^{1}H-NMR (500 MHz, $CDCl_3$) δ (ppm) 4.87 (quin, J = 7.4 Hz, 1H), 3.36 (t, J = 7.4 Hz, 2H), 1.70

(quin, J = 7.4 Hz, 2H), 1.63 (d, J = 7.4 Hz, 3H), 1.40 (br quin, J = 7.2 Hz, 2H), 1.26 (br, 16H), 0.88 (t, J = 6.9 Hz, 3H).

Synthesis of 1-(6-isocyanatohexyl)-3-(6-methyl-4-oxo-1,4- dihydropyrimidin-2-yl)urea (UPyNCO)

UPyNCO was synthesized using a protocol outlined in the literature.[30] The compound was confirmed by ^{1} H-NMR in agreement with the literature.[30] ^{1}H-NMR (300 MHz, $CDCl_3$) δ ppm 13.10 (s, 1H), 11.86 (s, 1H), 10.17 (s, 1H), 5.82 (s, 1H), 3.28 (m, 4H), 2.23 (s, 3H), 1.62 (quin, J = 6.9 Hz, 4H), 1.41 (m, 4H)

Synthesis of 2-(((6-(3-(6-methyl-4-oxo-1,4-dihydropyrimidin-2-yl) ureido)hexyl)carbamoyl)oxy)ethyl methacrylate (UPyMA)

The synthesis of UPyMA followed the method outlined in the literature.[30] UPyMA was confirmed by ^{1}H-NMR, in agreement with the literature (Figure S2).[30] ^{1}H-NMR (300 MHz, $CDCl_3$) δ ppm 13.13 (s, 1H), 11.86 (s, 1H), 10.07 (s, 1H), 6.14 (m, 1H), 5.86 (m, 1H), 5.60 (m, 1H), 5.00 (br, 1H), 4.32 (m, 4H), 3.25 (quart, J = 5.8 Hz, 2H), 3.17 (m, 2H), 2.23 (s, 3H), 1.94 (s, 3H), 1.62 (m, 2H), 1.58 (m, 2H), 1.50 (m, 4H).

Synthesis of furfuryl methacrylate (FMA)

The synthesis of FMA followed the method reported in the literature.[29] FMA was confirmed by ^{1}H-NMR, in agreement with the literature (Figure S3).[29] ^{1}H-NMR (300 MHz, $CDCl_3$) δ ppm 7.42 (s, 1H), 6.42 (d, J = 3.2 Hz, 1H), 6.40–6.33 (m, 1H), 6.13 (s, 1H), 5.57 (s, 1H), 5.13 (s, 2H), 1.94 (s, 3H).

Typical synthesis of PEA-UPyMA-FMA Materials by RAFT Polymerization.

Synthesis of PEA_{100}-$UPyA_{3.75}$-$FMA_{3.75}$ is presented here to demonstrate the general procedure of RAFT polymerization. Other materials were synthesized by a similar approach. To a round

bottom containing a magnetic stirrer bar, ethyl acrylate (EA) (5.00 g, 0.0499 mol), FMA (0.2490 g, 0.001498 mol), UPyMA (0.6341 g, 0.001497 mol), PADTC (0.1401 g, 0.0003996 mol), AIBN (0.0066 g, 0.000041 mol), and DMF (10.6 mL) were added. The reaction mixture was homogenized. The reaction mixture was capped with a rubber septum and bubbled with nitrogen for 10 min to remove residual oxygen. The mixture was heated in an oil bath at 60 °C for 8 h. The reaction was targeted to 75–80% conversion of EA, determined by ^{1}H-NMR. The polymer was then precipitated from a solution of 50% hexanes and 50% diethyl ether, and the polymer was dried in a vacuum oven. The polymer was dissolved in 6.16 mL of DMF, and 1,1′-(methylenedi-4,1-phenylene) bismaleimide (BMI) (0.3221 g, 0.0009 mol) was dissolved in 2.12 mL DMF. The dissolved polymer was mixed with the BMI solution, and the solution was transferred to Teflon molds and heated at 50–55 °C for 48 h. After the polymer had crosslinked, the materials were removed from the Teflon molds and allowed to dry in the fume hood for 2 days and overnight in a vacuum oven.

Synthesis of PEA-UPyMA-FMA polymer via conventional radical polymerization

In a round bottom equipped with a magnetic stirrer bar, ethyl acrylate (EA) (5.00 g, 0.0499 mol), FMA (0.2490 g, 0.001498 mol), UPyMA (0.6341 g, 0.001497 mol), AIBN (0.0066 g, 0.000041 mol), dodecanethiol (0.5050 g, 0.0025 mmol) were mixed with 10 g of DMF to obtain a homogenized mixture. The reaction mixture was then purged with nitrogen for 10 min and heated at 65 °C for 3.5 hrs. After 3.5 hrs, the conversion of EA was determined by ^{1}H-NMR (~80%). The obtained polymer was purified by precipitating with 50-50% Ethanol-water solvent mixture. The polymer was crosslinked following the same procedure as the materials synthesized by RAFT.

Characterization methods

All nuclear magnetic resonance (NMR) were performed in $CDCl_3$ using a Bruker 300 MHz or 500 MHz spectrometer. Number average molecular weights were determined as outlined in the literature.[29] All Infrared (IR) spectra were collected using a PerkinElmer Spectrum 100 Spectrometer.

Differential scanning calorimetry (DSC)

DSC was performed on a TA Instruments Q20 system, with a heat–cool–heat cycle ranging from −40 °C to +195 °C at a heating rate of 10 °C min^{-1}. Only data from the second heating cycle was used. The glass transition temperature (T_g) was determined as the inflection point of the 5-point averaged smoothed second heating cycle.

Size Exclusion Chromatography (SEC)

Polymer molecular weight distributions and dispersities were determined using an Agilent 1260 SEC system equipped with an autosampler, a degasser, an Agilent 1260 isocratic pump, 1 Agilent guard and 2 Agilent analytical Polar Gel-M columns and an Agilent 1260 refractive index (RI detector). N,N-Dimethylformamide (DMF) + 0.1 wt% LiBr was used as the eluent at a flow rate of 1 mL min^{-1} at 50 °C. Each sample was filtered before injection. Poly(methyl methacrylate) standards were used as calibrants in the SEC system.

Tensile testing

All tensile tests were performed on an Instron 3344 universal testing system equipped with a 100 N load cell. The extension was increased at the rate of 1 mm s^{-1} and all samples were measured until the material broke.

Cutting and healing procedures

Materials were cut into half with a razor blade. The halves were then placed in contact together. The reattached materials were placed either in a preheated oven at 80 °C or on a non-stick pan at ambient temperature.

Stress relaxation test

An Instron 3344 apparatus equipped with a 100 N load cell was used to analyze stress relaxation in an ambient environment. The extension was increased at the rate of 0.5 mm s^{-1} until 25% of the average strain at break for each material was achieved. The strain was maintained for 4 hours while the stress was measured.

Rheology

A TA instruments Discovery HR-1 rheometer was used for all rheological experiments. A 20 mm crosshatched parallel plate geometry was used at 0.1% applied strain for rheological frequency sweeps. 0.1 Hz frequency was used for the temperature sweep.

Long-term stability and creep recovery

A specimen of known length was stretching to 25% of the average strain at break for that material under ambient conditions for 24 h. After 24 hours, the strain was released and the material length was measured at over time. Creep recovery is determined by comparing the strained length to the original length.

Results and Discussion

Single network (SN) polymer materials were synthesized using RAFT polymerization. The advantages of the RAFT approach is that the chain length of a polymer can be tailored by monomer feed or by a ratio of monomer to RAFT chain transfer agent (CTA).[45] The single network materials can be synthesized by a simple one-pot polymerization. Both the hydrogen-

bonded UPyMA units and the precursors to the Diels-Alder furan-maleimide linkages are incorporated into the same backbone. The pendant furan units on the polymers were subsequently crosslinked using 1,1′-(methylenedi-4,1-phenylene) bismaleimide (BMI). The polymers are synthesized as outlined in Scheme 1. Due to the need to precipitate polymers after polymerization, methacrylic monomers were chosen to promote the incorporation of the functional FMA and UPyMA units and minimize any FMA or UPyMA units not incorporated into the materials. Due to the poor solubility of UPy based monomers in many solvents, it would be very difficult to separate unreacted UPy based monomer and the polymer. The UPyMA monomer is more reactive than the EA backbone forming monomer, hence UPyMA is preferentially incorporated into the polymer, and that at the end of the polymerization there is minimal unreacted UPy based monomer to complicate polymer purification.

The number average molecular weight (M_n) of the PEA-UPyMA-FMA polymers were determined by NMR, and the molar mass dispersity (M_w/M_n) were determined by SEC. These molecular weight data are given in Table 1. Two key parameters were varied; the crosslink density was varied at chain length or degree of polymerization (DP) of 100 units of EA from 2.5 mol% to 3.75 mol% to 5 mol% of each linker. Note the targeted molar amount of FMA equaled the targeted amount of UPyMA. In the second case, the total density of crosslinkers was kept constant, but the chain length was varied between 50 and 150 units. Additionally, two control materials were synthesized. One control used RAFT targeting a chain length of 100 units and 10 units of crosslinker, however, only the dynamic covalent FMA based linker was included. This material is labeled PEA_{100}-$UPyMA_0$-FMA_{10}. Further to investigate the impact of dispersity a conventional free radical based polymerization using 1-dodecanethiol as the transfer agent was used. This material targeted 3.75% of UPyMA and 3.75% of FMA and is labeled as PEA_{100}-

$UPyMA_{3.75}$-$FMA_{3.75}$-FRP, although it is noted the high dispersity of the material makes this type of label underestimate the variability in chain lengths and compositions, but instead is targeted to the idea of 3.75% of each linker. The molecular weight data are given in Table 1. Processed NMR spectra of the polymers are given in Figures S4-S10, with the SEC traces of all polymers synthesized given in Figure S11.

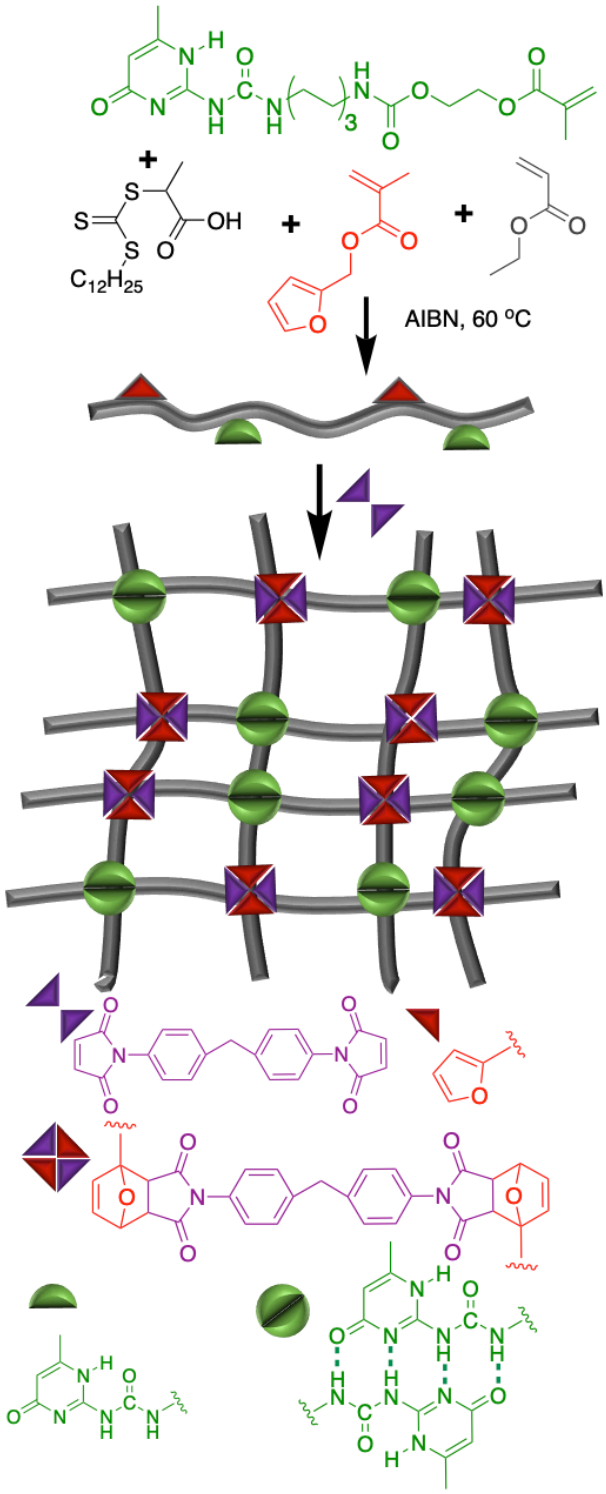

Scheme 1. Synthesis of PEA-UPyMA-FMA polymers by RAFT and their crosslinking using BMI.

Table 1: Molecular weight, dispersity and compositional properties of RAFT polymers used to synthesize single networks. [a] M_n and number average units were calculated by NMR, [b] M_w/M_n was calculated by SEC.

Entry	Polymer	M_n[a]	M_w/M_n[b]	Units UPyMA[a]	Units FMA[a]	Units EA[a]
1	PEA_{100}-$UPyMA_{2.5}$-$FMA_{2.5}$	12000	1.17	2.8	2.7	98
2	PEA_{100}-$UPyMA_{5}$-FMA_{5}	12000	1.24	5.6	4.4	84
3	PEA_{50}-$UPyMA_{1.9}$-$FMA_{1.9}$	5900	1.23	2.2	1.7	43
4	PEA_{100}-$UPyMA_{3.75}$-$FMA_{3.75}$	14000	1.38	4.4	3.7	110
5	PEA_{150}-$UPyMA_{5.6}$-$FMA_{5.6}$	18000	1.38	6	4.8	145
6	PEA_{100}-$UPyMA_{0}$-FMA_{10}	12000	1.38	0	11.5	93
7	PEA_{100}-$UPyMA_{3.75}$-$FMA_{3.75}$-FRP	9500	2.4	2.8	2.6	77

Covalent crosslinking of polymers was performed using BMI to react with pendant furan units through Diels-Alder chemistry, with the UPy units undergoing spontaneous dimerization through hydrogen bonding. The material properties were evaluated. Table 2 gives the average thermal and mechanical properties of each system. Differential scanning calorimetry (DSC) was used to determine the glass transition temperature (T_g) of each polymer. Increasing either crosslink density or chain length increases T_g. As indicated in Table 2, PEA_{100}-$UPyMA_{2.5}$-$FMA_{2.5}$ with T_g = -16.43 °C increases to T_g = 9.00 °C for PEA_{100}-$UPyMA_5$-FMA_5, and PEA_{50}-$UPyMA_{1.9}$-$FMA_{1.9}$ with T_g = -6.23 °C increases to T_g = 2.93 °C for PEA_{150}-$UPyMA_{5.6}$-$FMA_{5.6}$. High crosslink density and long chain lengths create restrictions on the polymer backbone movements, implying that more thermal energy is needed to relax the backbone and cross the glass transition. Typical DSC traces are given in Figure S12. An IR spectrum of the PEA_{100}-$UPyMA_{3.75}$-$FMA_{3.75}$ materials, after extraction from the molds and drying in a vacuum oven, is

given in Figure S13. The IR spectrum of the EA based material agrees with those reported for other poly(EA) based networks.

Table 2: Thermal and mechanical properties of RAFT synthesized polymer single networks based on PEA-UPyMA-FMA. Uncertainties represent standard errors of the mean.

Entry	Polymer	T_g (°C)	T_{cross} (°C)	σ_{peak} (kPa)	ε_{break} (mm/mm)	E (kPa)
1	PEA_{100}-$UPyMA_{2.5}$-$FMA_{2.5}$	-16.43	80	260 ± 30	3.4±0.2	390 ± 60
2	PEA_{100}-$UPyMA_{5}$-FMA_{5}	9.00	100	1400 ± 300	1.3 ± 0.2	2600 ± 400
3	PEA_{50}-$UPyMA_{1.9}$-$FMA_{1.9}$	-6.23	70	-	-	-
4	PEA_{100}-$UPyMA_{3.75}$-$FMA_{3.75}$	-0.25	90	1500 ±200	2.8 ± 0.2	1100 ± 100
5	PEA_{150}-$UPyMA_{5.6}$-$FMA_{5.6}$	2.93	115	1700 ± 200	1.7 ± 0.1	2400 ± 200

All PEA-UPyMA-FMA materials were analyzed via rheology. Figure S14 gives strain sweep data for the PEA_{100}-$UPyMA_{3.75}$-$FMA_{3.75}$ material. The strain sweep data indicates that the linear viscoelastic region holds beyond 0.1% applied strain, therefore for all subsequent rheological experiments a strain of 0.1% was applied. Frequency sweeps at 25 °C and 0.1% strain at room temperature for all materials indicate similar storage and loss moduli that increase along with increasing frequency as the material approaches the glass transition. Storage moduli for all materials approach a nearly flat, linear region before the approach to the glass transition indicating a rubber-like material. These frequency sweep data are given in Figures S15-S19.

Temperature sweeps were performed at 0.1 Hz and 0.1% strain from 20 °C to 120 °C. As temperature increases, the storage and loss moduli decrease. The systems transition from an elastic rubber-like nature at 20 °C or slightly above to a viscous one as the crossover point between the storage and loss moduli is reached for each material. The temperatures at the

crossover points for the PEA-UPyMA-FMA materials are given in Table 2. An increase in crosslink density necessitates an increase in temperature to dissociate a critical fraction of the Diels-Alder bonds to allow the materials to flow. Similarly, systems with larger chain lengths result in higher crossover temperatures. Longer chain systems require higher temperatures due to a larger number of elastically effective Diels-Alder bonds that must dissociate for the material to transition from a viscoelastic solid to a liquid. These temperatures are consistent with the temperature range at which the Diels-Alder bonds in the systems dissociate.[55]

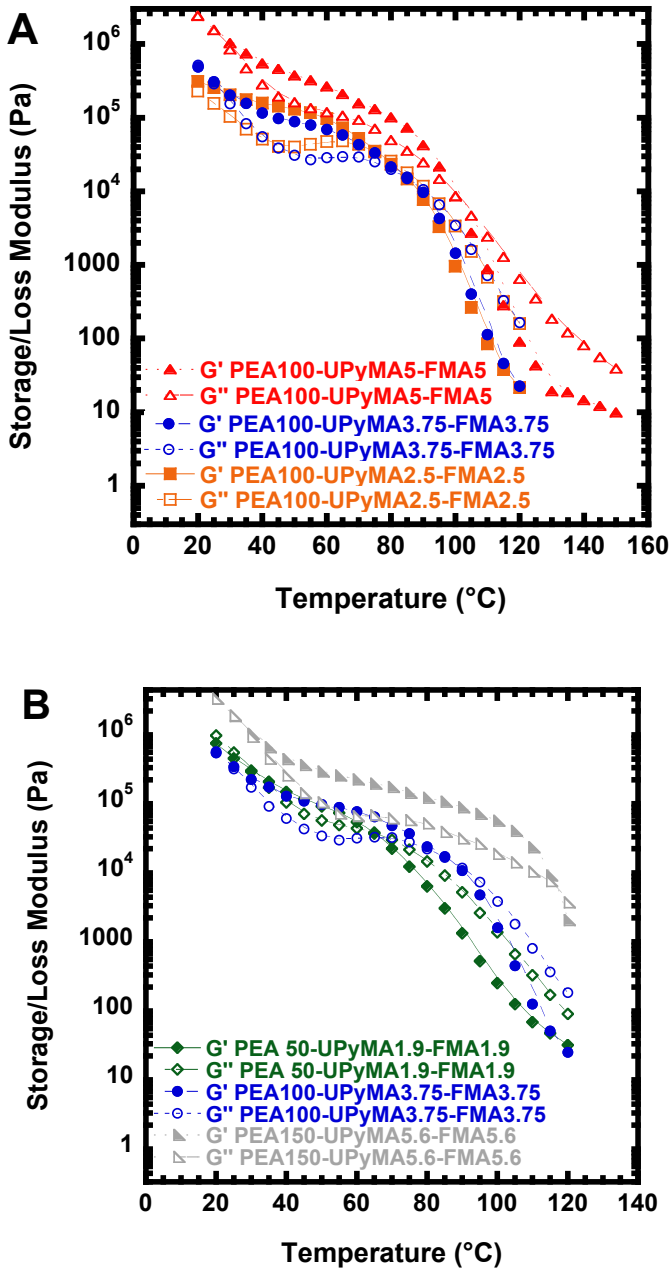

Figure 1 (A) Temperature sweep rheological data showing storage and loss moduli for PEA-UPyMA-FMA materials with DP 100 using 0.1% strain and 0.1 Hz. (B) Temperature sweep rheological data showing storage and loss moduli for PEA-UPyMA-FMA materials with different chain lengths using 0.1% strain and 0.1 Hz.

The mechanical properties of the PEA-UPyMA-FMA single network materials, as well as the two controls, were also examined. As indicated in Figure 2, networks based on longer chain

lengths or higher crosslink densities had higher peak stress (σ_{peak}) values but lower strain at break (ε_{break}). Typical variability of uncut stress-strain curves for all materials except for PEA_{50}-$UPyMA_{1.9}$-$FMA_{1.9}$ can be found in Figures S20-25. PEA_{50}-$UPyMA_{1.9}$-$FMA_{1.9}$ exhibited yielding and plastic deformation-like behavior, and reliable tensile data could not be acquired for the material. Each dual dynamic RAFT material's Young's modulus (E) was determined by fitting the Ogden model.[29,56] In fitting the experimental data to the Ogden model, only the data up to the peak stress were used. Fitted Young's modulus curves to all dual dynamic RAFT materials are given in Figure S26. Interestingly, the PEA_{100}-$UPyMA_{3.75}$-$FMA_{3.75}$ and PEA_{100}-$UPyMA_{5}$-FMA_{5} reached a peak stress (σ_{peak}) of approximately 1.5 MPa, while PEA_{150}-$UPyMA_{5.6}$-$FMA_{5.6}$ reached a σ_{peak} of 2 MPa. Although these values are high, compared to earlier developed materials synthesized by one pot conventional radical polymerization, they are notably smaller than the values reached by IPN materials of similar composition.[29–31] Conversely, the PEA_{100}-$UPyMA_{2.5}$-$FMA_{2.5}$ exhibited yielding and plastic deformation behavior during testing after reaching a peak, presumably due to poor network percolation due to low crosslink density, which causes poor network structure. Further, the hydrogen-bonded UPyMA units could exchange on the timescale of the tensile test, leading to some creep or yielding behavior. The Young's moduli data are consistent with the trends in σ_{peak} and ε_{break}, with the materials having higher crosslink density or longer chain lengths having a larger value of E. The control material PEA_{100}-$UPyMA_{0}$-FMA_{10} reached very high stress values of over 3 MPa, due to the high density of covalent crosslinks, although at the cost of elasticity, with the materials breaking before a strain 1 was applied, as seen in Figure S24. Similarly the PEA_{100}-$UPyMA_{3.75}$-$FMA_{3.75}$-FRP material performed poorer than the PEA_{100}-$UPyMA_{3.75}$-$FMA_{3.75}$ material made by RAFT. The PEA_{100}-$UPyMA_{3.75}$-$FMA_{3.75}$ material made by FRP reached substantially lower strain values and

somewhat lower stress values than the comparable material made by RAFT, as is evident in comparing Figures S22 for the RAFT materials and S25 for the FRP materials.

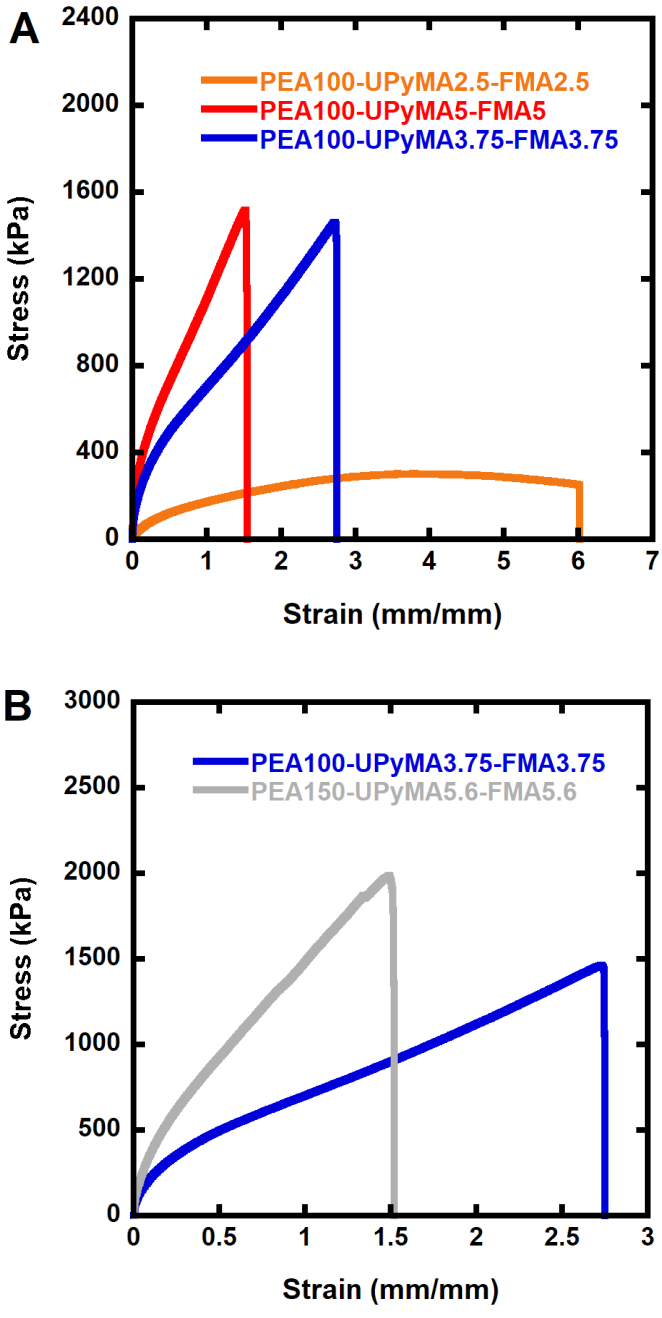

Figure 2 (A) Typical stress–strain curves of materials with different crosslink densities. (B) Typical stress–strain curves of materials with different backbone chain lengths.

The presence of dynamic bonds enables self-healing in the polymer materials. Self-healing tests are performed by cutting materials into halves, and then reattaching the halves. The materials are then incubated at either ambient temperature or 80 °C for given time frames. Since Diels-Alder bonds require thermal stimuli for dynamic covalent exchange, ambient self-healing results only in reformation of the UPyMA hydrogen crosslinkers, whereas heated self-healing results in the reformation of both UPyMA and Diels-Alder bonds. Therefore, the focus of self-healing studies in this work is the healing at elevated temperatures (80 °C). In general the materials did not show consistent self-healing under ambient conditions over a 10-minute time frame, although longer times could lead to self-healing.[29] This is different to the IPN materials which showed good self-healing over this 10 min timeframe, even at room temperature, and this is most likely due to the IPN material having greater freedom and the ability to create a larger number of non-covalent linkages that are needed for room temperature self-healing, as indicated by molecular dynamics simulations.[18,29] The self-healing ability of PEA_{100}-$UPyMA_5$-FMA_5 at elevated temperature (80 °C) is shown in Figure 3. The 8-hour mark indicates approximately 50% recovery in both peak stress and strain of the material, and the 24-hour mark an almost complete recovery.

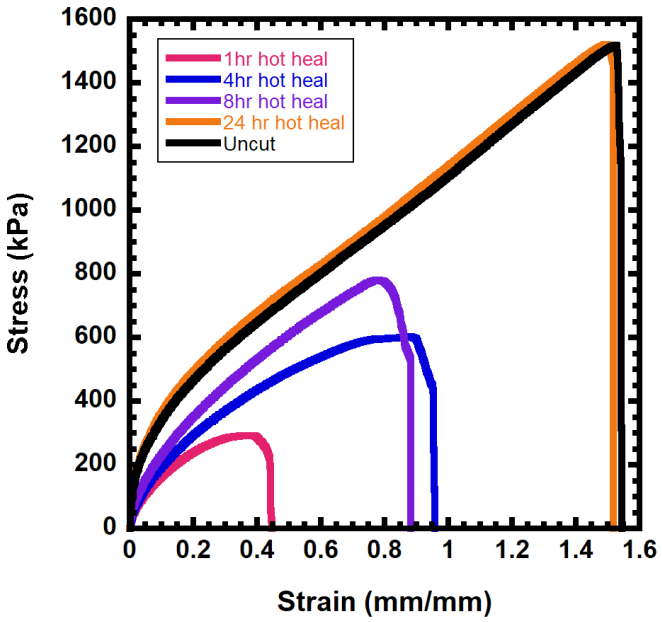

Figure 3 Stress–strain curves of PEA_{100}-$UPyMA_5$-FMA_5 for a 1 hour, 4 hour, 8 hour, 24 hour hot healing periods and an uncut sample.

Figures S27-28 show the self healing performance of the PEA_{100}-$UPyMA_{3.75}$-$FMA_{3.75}$ and PEA_{150}-$UPyMA_{5.6}$-$FMA_{5.6}$ based materials. 80 °C healed stress strain curves for all non-yielding materials indicated that for the 4-hour time frame, PEA_{100}-$UPyMA_{3.75}$-$FMA_{3.75}$ had the best self-healing properties, with a ~50% recovery in peak stress and ~60% recovery in strain at break. These recoveries are similar for PEA_{100}-$UPyMA_5$-FMA_5 with a ~43% recovery in peak stress and ~53% recovery in strain at break, and PEA_{150}-$UPyMA_{5.6}$-$FMA_{5.6}$ with a ~37% recovery in peak stress and ~40% recovery in strain at break. For PEA_{100}-$UPyMA_{3.75}$-$FMA_{3.75}$ and PEA_{100}-$UPyMA_5$-FMA_5, heating periods of 24 hours result in >95% recovery in peak stress and >95% recovery in strain at break. PEA_{150}-$UPyMA_{5.6}$-$FMA_{5.6}$ exhibited ~80% recovery in peak stress and ~93% recovery in strain at break after 16 hours. Figure S29 shows the yielding behavior of PEA_{100}-$UPyMA_{2.5}$-$FMA_{2.5}$. Table S1 summarizes the self-healing performance of the materials.

Further, the PEA_{100}-$UPyMA_{0}$-FMA_{10} control material, which only contained the dynamic covalent bonds, did not show any self-healing even after being heated at 80 °C for 24 h, unlike the PEA_{100}-$UPyMA_{5}$-FMA_{5} that had excellent self-healing in this same time frame. This would suggest that having the same total crosslink density, but replacing the hydrogen bonded UPy linkers with dynamic covalent linkers is detrimental to the material's mechanical properties. This suggests a synergy between the dynamic covalent and dynamic non-covalent linkers, where the dynamic non-covalent linkers could help associate the two parts of the material rapidly and facilitate dynamic covalent exchange. Similarly, comparison of the dynamic properties of the PEA_{100}-$UPyMA_{3.75}$-$FMA_{3.75}$-FRP material to the PEA_{100}-$UPyMA_{3.75}$-$FMA_{3.75}$ material made by RAFT in Figure 4 suggests that the primary polymer structure is also important to dynamic exchange and self-healing. In FRP there are likely many short chains which are unable to percolate into the macroscopic network effectively, despite these polymers having high diffusivity, and at the same time FRP produces many very high molecular weight polymers which have poor diffusivity and limited dynamic exchange potential. In contrast, RAFT leads to polymers of similar molecular weights, leading to superior self-healing and overall mechanical performance. This highlights the importance of controlling the primary chain's properties through processes such as RAFT.

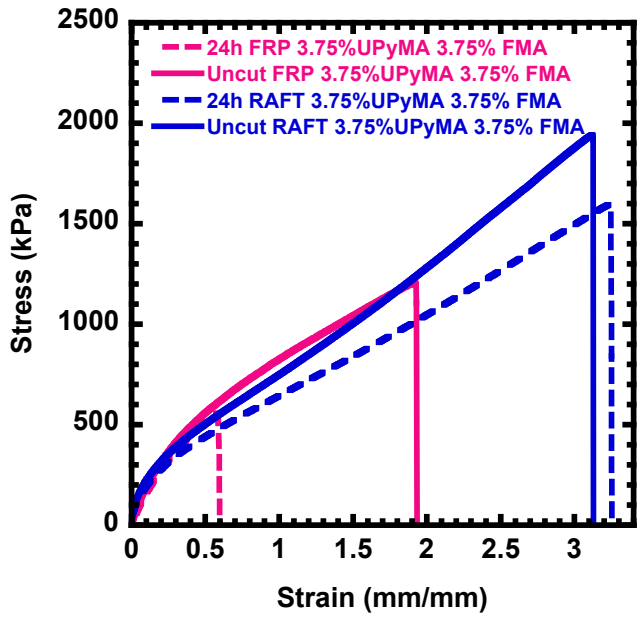

Figure 4 Self-healing properties of PEA_{100}-$UPyMA_{3.75}$-$FMA_{3.75}$ materials made by FRP compared to PEA_{100}-$UPyMA_{3.75}$-$FMA_{3.75}$ materials made by RAFT at 80 °C.

Despite the hydrogen bonds typically leading to minimal room temperature self-healing for many materials, the presence of hydrogen bonds can dissipate energy and increase toughness. Stress relaxation experiments were performed by straining each material to 25% of that materials average strain at break. Experiments were not performed for PEA_{50}-$UPyMA_{1.9}$-$FMA_{1.9}$ because the material was soft and gave poor tensile data, making it difficult to accurately measure stress relaxation. As indicated in Figure 5A, each material had excellent stress relaxation properties. The stress relaxation was essentially complete for PEA_{100}-$UPyMA_{2.5}$-$FMA_{2.5}$ and greater than 95% for the other materials. The presence of exchangeable and dynamic hydrogen bonds enables this excellent stress relaxation in the polymer networks. However, the stress relaxation was fastest for the materials with the lowest Young's modulus. This suggests that in these SN materials the presence of many essentially static covalent crosslinkers decreases relaxation and reduces the rate of stress relaxation.

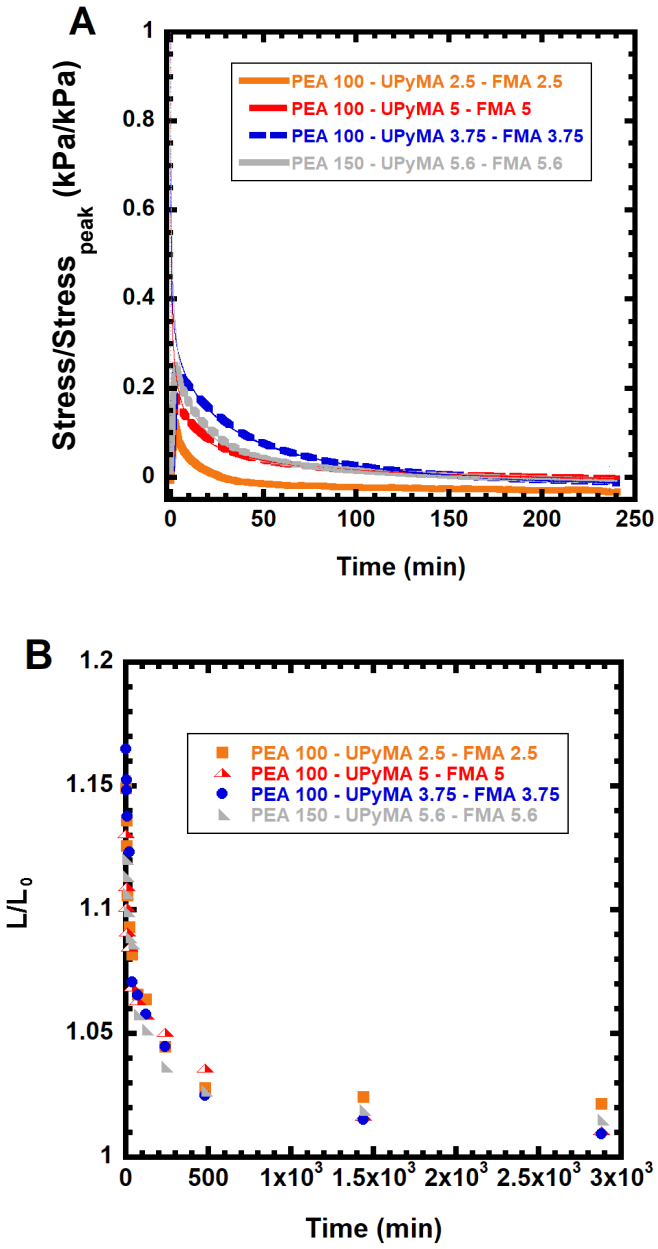

Figure 5 (A) Stress relaxation of all PEA-UPyMA-FMA materials. Materials were strained to the 25% average strain at break. (B) Creep recovery as a function of time for all the materials after being released from the 25% average strain at break. Both studies were performed at ambient temperature.

Resistance to creep deformation is a desirable material trait. Stability was tested by subjecting the materials to stress relaxation and creep recovery as described in Figure 5B. All materials were strained to 25% of their respective average ε_{break} and fixed at room temperature. After 4 hours, the strain was released and the material began to recover. Lengths of the materials at certain time intervals were recorded and plotted in Figure 5B. All tested materials exhibited >95% length recovery after 24 hours. This is important for applications of these materials in high stress environments, since despite the materials having excellent stress relaxation properties, the induced creep is not permanent and the overall materials permanent shape is maintained through covalent bonds.

Conclusions

Single network polymer materials containing hydrogen-bonded UPyMA units and dynamic covalent furan-maleimide based crosslinkers were synthesized via RAFT polymerization. RAFT allows precision control over polymer synthesis enabling the chain length or crosslink density to be tuned in material composition. Higher crosslink densities and longer chain lengths lead to stronger materials with less elasticity. Low crosslink densities and short chain lengths resulted in materials that yielded. Materials exhibited a rheological crossover temperature in the range of 70-115 °C, transitioning from a viscoelastic solid to a viscoelastic liquid at that temperature. Increasing either crosslink density or chain length results in a higher crossover temperature. Materials with at least a chain length of 100 or 3.75 mol% crosslinker density exhibited self-healing properties. Materials below this threshold exhibited yielding or plastic deformation during tensile testing. The materials also relax stress to near complete recovery due to the exchange of H bonded UPyMA units. They also exhibit creep resistance. Such properties indicate that the materials have applications as next generation coating, sealants, or elastomers.

Acknowledgements

We thank Progyateg Chakma for assistance with the FMA synthesis, and Obed Dodo for assistance with UPyMA synthesis. This material is based upon work supported by the National Science Foundation under Grant No. (DMR-1749730). Acknowledgment is also made to the Donors of the American Chemical Society under Petroleum Research Fund (57243-DNI7) for partial support of this work. HL acknowledges support from the National Science Foundation under Grant No. (CHE-1460862) under the REU site in chemistry at Miami University. Dominik Konkolewicz would also like to acknowledge support from the Robert H. and Nancy J. Blayney Professorship.

References:

1 R. J. Wojtecki, M. A. Meador and S. J. Rowan, *Nat. Mater.*, 2011, **10**, 14–27.

2 B. J. Blaiszik, S. L. B. Kramer, S. C. Olugebefola, J. S. Moore, N. R. Sottos and S. R. White, *Annu. Rev. Mater. Res.*, 2010, **40**, 179–211.

3 N. Kuhl, S. Bode, M. D. Hager and U. S. Schubert, *Self-Healing Materials*, Springer, Berlin, 1st edn., 2016.

4 A. Chao, I. Negulescu and D. Zhang, *Macromolecules*, 2016, **49**, 6277–6284.

5 Z.-C. Jiang, Y.-Y. Xiao, Y. Kang, M. Pan, B.-J. Li and S. Zhang, *ACS Appl. Mater. Interfaces*, 2017, **9**, 20276–20293.

6 X.-J. Zhang, Q.-S. Yang, X. Liu, J.-J. Shang and J.-S. Leng, *Smart Mater. Struct.*, 2019, **29**, 15040.

7 Q. Meng and J. Hu, *J. Appl. Polym. Sci.*, 2008, **109**, 2616–2623.

8 F. Lancia, A. Ryabchun, A.-D. Nguindjel, S. Kwangmettatam and N. Katsonis, *Nat. Commun.*, 2019, **10**, 4819.

9 P. Chakma and D. Konkolewicz, *Angew. Chemie Int. Ed.*, 2019, **58**, 9682–9695.

10 M. A. C. Stuart, W. T. S. Huck, J. Genzer, M. Müller, C. Ober, M. Stamm, G. B.

Sukhorukov, I. Szleifer, V. V Tsukruk, M. Urban, F. Winnik, S. Zauscher, I. Luzinov and S. Minko, *Nat. Mater.*, 2010, **9**, 101–113.

11 L. Voorhaar and R. Hoogenboom, *Chem. Soc. Rev.*, 2016, **45**, 4013–4031.

12 X. Zhang, W. Xi, C. Wang, M. Podgórski and C. N. Bowman, *ACS Macro Lett.*, 2016, **5**, 229–233.

13 D. Apostolides and C. Patrickios, *Polym. Int.*, 2018, **67**, 627–649.

14 J. J. Cash, T. Kubo, D. J. Dobbins and B. S. Sumerlin, *Polym. Chem.*, 2018, **9**, 2011–2020.

15 S. D. Fontaine, R. Reid, L. Robinson, G. W. Ashley and D. V Santi, *Bioconjug. Chem.*, 2015, **26**, 145–152.

16 Y. Jin, Q. Wang, P. Taynton and W. Zhang, *Acc. Chem. Res.*, 2014, **47**, 1575–1586.

17 P. Wang, G. Deng, L. Zhou, Z. Li and Y. Chen, *ACS Macro Lett.*, 2017, **6**, 881–886.

18 M. B. Zanjani, B. Zhang, B. Ahammed, J. P. Chamberlin, P. Chakma, D. Konkolewicz and Z. Ye, *Macromol. Theory Simulations*, 2019, **28**, 1900008.

19 S. Kubik, *Angew. Chemie Int. Ed.*, 2018, **57**, 3005.

20 C. J. Kloxin, T. F. Scott, B. J. Adzima and C. N. Bowman, *Macromolecules*, 2010, **43**, 2643–2653.

21 C. N. Bowman and C. J. Kloxin, *Angew. Chemie Int. Ed.*, 2012, **51**, 4272–4274.

22 Y. Deng, I. Hussain, M. Kang, K. Li, F. Yao, S. Liu and G. Fu, *Chem. Eng. J.*, 2018, **353**, 900–910.

23 S. M. Mantooth, B. G. Munoz-Robles and M. J. Webber, *Macromol. Biosci.*, 2019, **19**, 1800281.

24 W.-H. Hsu, Y.-C. Kao, S.-H. Chuang, J.-S. Wang, J.-Y. Lai and H.-C. Tsai, *RSC Adv.*, 2019, **9**, 24241–24247.

25 R. P. Sijbesma and E. W. Meijer, *Chem. Commun.*, 2003, 5–16.

26 S. Oka, H. Ozawa, K. Yoshikawa, T. Ikeda and M. Haga, *Dalt. Trans.*, 2018, **47**, 14195–14203.

27 T. T. T. Myllymäki, A. Guliyeva, A. Korpi, M. A. Kostiainen, V. Hynninen, Nonappa, P. Rannou, O. Ikkala and S. Halila, *Chem. Commun.*, 2019, **55**, 11739–11742.

28 C. E. Diesendruck, N. R. Sottos, J. S. Moore and S. R. White, *Angew. Chemie Int. Ed.*, 2015, **54**, 10428–10447.

29 B. Zhang, J. Ke, J. R. Vakil, S. C. Cummings, Z. A. Digby, J. L. Sparks, Z. Ye, M. B. Zanjani and D. Konkolewicz, *Polym. Chem.*, 2019, **10**, 6290–6304.

30 B. Zhang, Z. A. Digby, J. A. Flum, E. M. Foster, J. L. Sparks and D. Konkolewicz, *Polym. Chem.*, 2015, **6**, 7368–7372.

31 E. M. Foster, E. E. Lensmeyer, B. Zhang, P. Chakma, J. A. Flum, J. J. Via, J. L. Sparks and D. Konkolewicz, *ACS Macro Lett.*, 2017, **6**, 495–499.

32 P. Du, M. Wu, X. Liu, Z. Zheng, X. Wang, T. Joncheray and Y. Zhang, *J. Appl. Polym. Sci.*, , DOI:10.1002/app.40234.

33 F. Yu, X. Cao, J. Du, G. Wang and X. Chen, *ACS Appl. Mater. Interfaces*, 2015, **7**, 24023–24031.

34 Y.-L. Liu and T.-W. Chuo, *Polym. Chem.*, 2013, **4**, 2194–2205.

35 Y. Zhong, X. Wang, Z. Zheng and P. Du, *J. Appl. Polym. Sci.*, , DOI:10.1002/app.41944.

36 X. Kuang, G. Liu, X. Dong and D. Wang, *Macromol. Mater. Eng.*, 2016, **301**, 535–541.

37 P. A. Pratama, M. Sharifi, A. M. Peterson and G. R. Palmese, *ACS Appl. Mater. Interfaces*, 2013, **5**, 12425–12431.

38 J. S. Park, T. Darlington, A. F. Starr, K. Takahashi, J. Riendeau and H. Thomas Hahn,

Compos. Sci. Technol., 2010, **70**, 2154–2159.

39 L. Yang, X. Lu, Z. Wang and H. Xia, *Polym. Chem.*, 2018, **9**, 2166–2172.

40 A. M. Peterson, R. E. Jensen and G. R. Palmese, *ACS Appl. Mater. Interfaces*, 2010, **2**, 1141–1149.

41 P. Du, X. Liu, Z. Zheng, X. Wang, T. Joncheray and Y. Zhang, *RSC Adv.*, 2013, **3**, 15475–15482.

42 P. Reutenauer, E. Buhler, P. J. Boul, S. J. Candau and J.-M. Lehn, *Chem. – A Eur. J.*, 2009, **15**, 1893–1900.

43 P. J. Boul, P. Reutenauer and J.-M. Lehn, *Org. Lett.*, 2005, **7**, 15–18.

44 A. J. Inglis, L. Nebhani, O. Altintas, F. G. Schmidt and C. Barner-Kowollik, *Macromolecules*, 2010, **43**, 5515–5520.

45 S. Perrier, *Macromolecules*, 2017, **50**, 7433–7447.

46 G. Moad, *Polym. Chem.*, 2017, **8**, 177–219.

47 C. H. Hornung, C. Guerrero-Sanchez, M. Brasholz, S. Saubern, J. Chiefari, G. Moad, E. Rizzardo and S. H. Thang, *Org. Process Res. Dev.*, 2011, **15**, 593–601.

48 J. Ferreira, J. Syrett, M. Whittaker, D. Haddleton, T. P. Davis and C. Boyer, *Polym. Chem.*, 2011, **2**, 1671–1677.

49 Q. Fu, H. Ranji-Burachaloo, M. Liu, T. G. McKenzie, S. Tan, A. Reyhani, M. D. Nothling, D. E. Dunstan and G. G. Qiao, *Polym. Chem.*, 2018, **9**, 4448–4454.

50 J. D. Moskowitz, B. A. Abel, C. L. McCormick and J. S. Wiggins, *J. Polym. Sci. Part A Polym. Chem.*, 2016, **54**, 553–562.

51 Z. Jiang, A. Bhaskaran, H. M. Aitken, I. C. G. Shackleford and L. A. Connal, *Macromol. Rapid Commun.*, 2019, **40**, 1900038.

52 S. Cummings, O. J. Dodo, A. Hull, B. Zhang, C. Myers, J. L. Sparks and D. Konkolewicz, *ACS Appl. Polym. Mater.*, , DOI:10.1021/acsapm.9b01095.

53 W. L. Peng, Y. You, P. Xie, M. Z. Rong and M. Q. Zhang, *Macromolecules*, , DOI:10.1021/acs.macromol.9b02307.

54 A. F. Craig, E. E. Clark, I. D. Sahu, R. Zhang, N. D. Frantz, M. S. Al-Abdul-Wahid, C. Dabney-Smith, D. Konkolewicz and G. A. Lorigan, *Biochim. Biophys. Acta - Biomembr.*, 2016, **1858**, 2931–2939.

55 A. Buonerba, R. Lapenta, S. Ortega Sánchez, C. Capacchione, S. Milione and A. Grassi, *ChemistrySelect*, 2017, **2**, 1605–1612.

56 O. A. Shergold, N. A. Fleck and D. Radford, *Int. J. Impact Eng.*, 2006, **32**, 1384–1402.